Volume 15, Number 5, 2022. pp. 445-456

Jordan Journal of Physics

ARTICLE

Noise-dissipation Correlated Dynamics of a Double-well Bose-Einstein Condensate-reservoir System

Kalai K. Rajagopal, Gafurjan Ibragimov, Risman M. Hasim and **Idham A. Alias**

INSPEM & Department of Mathematics, University Putra Malaysia, 43400 Serdang, Selangor, Malaysia.

Doi: **https://doi.org/10.47011/15.5.2**

Received on: 31/12/2020; *Accepted on: 08/06/2021*

Abstract: In this work, we study the dissipative dynamics of a double-well Bose-Einstein condensate (BEC) out-coupled to reservoir at each side of its trap. The sub-system comprises of a simple Bose-Hubbard model, where the interplay of atom-tunneling current and inter-particle interaction are the main quantum features. The contact with two separate heat baths causes dissipation and drives the system into a non-equilibrium state. The system is well described by the Generalized Quantum Heisenberg-Langevin equation. We considered two Markovian dissipative BEC systems based on (i) the mean-field model (MF), where the internal noise has been averaged out and (ii) the noise-correlated model (FDT). Physical quantities, such as population imbalance, coherence and entanglement of the system, are computed for the models. The two-mode BEC phases, such as the quantum tunneling state and the macroscopic quantum-trapping state, evolved into complicated dynamics by controlling the non-linear interaction and dissipation strengths. We found that many important quantum features produced by the noise-correlated FDT model are not captured by the mean-field model.

Keywords: Double-well BEC, Dissipation, Noise, Markovian, Non-Markovian, Fixed points.

PACS: 03.75 Lm, 03.65 Yz, 03.75 Gg, 05.

1. Introduction

Bose-Einstein Condensate (BEC) in a double-well system exhibits quantum features mimicking the physics of Boson Josephson Junction (BJJ) dynamics in superconductors. Tunneling transport of atoms between the wells causes BEC population to oscillate even if there is no disparity between the number of atoms in each well, resulting in a modulated quantum collapse and revival; for instance, see [1, 2]. Macroscopic quantum coherence is then established within the system. However, stronger on-site boson-boson repulsive interaction suppresses the oscillations of population imbalance and goes upon a critical value, resulting in a novel macroscopic quantum self-trapping state, where atoms start localizing within their respective wells. This phenomenon is known as the Macroscopic Quantum Self-Trapping (MQST); for instance, see [2-4].

Experimental measurements, such as Josephson tunneling and thermal-induced phase fluctuations on the double-well BEC system, were reported in the monograph [5-7]. Measurements on the Josephson's AC and DC effects on the BJJ were made by Levy et al. [8] and interference-fringe experiments were performed by Hofferberth et al. [9]. Enormous

Corresponding Author: Kalai Kumar Rajagopal **Email**: kkrajagop@gmail.com

progress has been made following this experimental work.

System-environmental interaction under experimental conditions complicates the study of the transition from the quantum regime to the classical regime. Dissipation caused by irreversible coupling of quantum state with the environment creates a major obstacle in the long-time coherent control of quantum state. For a double-well BEC interacting with the environment setting, dissipation is found to be the major factor causing the destruction of MQST phases, as reported extensively in the theoretical literature [10-19]. On the contrary, researchers led by Sandro Wimberger [13, 15] have shown that dissipation in concurrence with inter-particle interaction enhances coherence under a specific condition. The double-well BEC is routinely realized with almost perfect control on atom-atom and external potential; for example in the experimental groups of Albiez et al. [5] and Gati et al. [6]. Resonance behaviour of coherence is anticipated to be realized in near future experiments. In the other direction, an experimental group led by Herwig Ott [20, 21, 47, 48] carried out a number of successful experiments applying localized dissipation to control the dynamic evolution of BEC, making this line of research very exciting.

Generally, inter-particle repulsive interaction [2-4, 14] cannot be neglected in any realistic BEC system. The physics of interacting BEC can be complicated in the presence of excitations. However, in this work, we neglect the existence of excitation, assuming weak-coupling approximation as in [22, 23]. In their works, two independent condensates having atoms in their lowest eigen-modes are merged and coherently out-coupled to their respective reservoirs. The interaction of condensate boson atoms in the traps with the reservoir induces dissipation in the system. The spectral function that couples the trap atoms with the reservoir modes determines the Markovian or non-Markovian operational dynamics of the system; see for instance [24-27].

Most studies on the dissipative double-well BEC-reservoir system encapsulate Markovian dynamics, leaving vast space for research on the non-Markovian operational basis. The emergence of new problems, such as quantum thermometry and quantum refrigerant [49, 50], led to many loopholes and excitement in this line of research. We follow the same motivation to explore our dissipative model of interest employing the generalized quantum Langevin equation (GQLE) which is discussed in great detail in the textbooks [22, 28, 30]. The advantage of using the latter mathematical approach is its feasibility to transform complicated stochastic differential equations into ordinary differential equations.

The paper is organized as follows. We describe the Hamiltonian of the double-well BEC-reservoir system by showing how it caters for Markovian or non-Markovian operational dynamics in Section 2. The Hamiltonian of the model and the dynamical equations can be found in our earlier works [29, 33]. Section 3 and its sub-section 3.1 discuss the mean-field model of our system. The system subjected to noise correlation and dissipation is described in Section 4. Results of the model physical quantities produced by the model are illustrated and discussed in the following sub-sections. A brief conclusion is given in Section 5.

2. Double-well BEC Out-coupled to Reservoirs

The Hamiltonian of the double-well BEC out-coupled to a dual multi-mode field (reservoirs) is succinctly denoted by the relation $H_{tot}=H_s+H_c+H_m+H_{s-c}+H_{s-m}$. The double-well (or two-mode) BEC sub-system is then represented by the sub-Hamiltonian:

$$H_s = \omega\ (\hat{a}^\dagger\ \hat{a} + \hat{b}^\dagger\ \hat{b}) + \Omega\ (\hat{a}^\dagger\ \hat{b} + \hat{b}^\dagger\ \hat{a}) + \mathrm{U}/2\ [\ \hat{a}^\dagger\ \hat{a}\ \hat{a}\ \hat{a} + b^\dagger\ \hat{b}\ \hat{b}\ \hat{b}\ ]. \quad (1)$$

Here, $(\hat{a}^\dagger,\ \hat{a})$ and $(\hat{b}^\dagger,\ \hat{b})$ are the set of creation and annihilation operators of the boson at traps A and B, respectively. Ω is the coupling strength between the two modes, ω is the trap frequency, U is the on-site interaction strength. We set $\hbar$=1; hence, all energies are measured in frequency units.

The two multi-mode reservoir fields are represented by $H_c = \sum_k \omega_k\ \hat{c}_k^\dagger\ \hat{c}_k$ and $H_m = \sum_k \omega_k\ \hat{m}_k^\dagger\ \hat{m}_k$, whereas they are connected at each side of the traps (A, B). The reservoirs are composed of closely spaced oscillators with frequencies ω_k with corresponding creation and annihilation operators $(\hat{c}_k^\dagger,\ \hat{c}_k)$ and $(\hat{m}_k^\dagger,\ \hat{m}_k)$. They are assumed to be in thermal equilibrium, satisfying:

$$\langle\ \hat{c}_k^\dagger\ (0)\ \rangle = \langle\ \hat{c}_k\ (0)\ \rangle = \langle \hat{m}_k^\dagger\ (0)\ \rangle = \langle\ \hat{m}_k\ (0)\ \rangle = 0$$

$\langle\, \hat{c}_k^\dagger\,(0)\, \hat{c}_{k'}(0)\,\rangle = \delta_{kk'}\, N_1(\omega_{k'})$

$\langle\, \hat{m}_k^\dagger\,(0)\, \hat{m}_{k'}(0)\,\rangle = \delta_{kk'}\, N_2\,(\omega_{k'})$

$\langle\, \hat{c}_k(0)\, \hat{c}_{k'}(0)\rangle = \langle\, \hat{m}_k(0)\, \hat{m}_{k'}(0)\rangle = 0$

$\langle \hat{c}_k^\dagger\,(0)\, \hat{c}_{k'}^\dagger(0)\rangle = \langle\, \hat{m}_k^\dagger\,(0)\, \hat{m}_{k'}^\dagger(0)\rangle = 0$

Here, $N_1(\omega)$ =1/[exp(ω/k_BT_1) – 1] and $N_2(\omega)$ =1/[exp(ω/k_BT_2) – 1] represent the thermal average boson numbers for reservoirs A and B, with Boltzmann constant k_B for temperatures (T_1, T_2), respectively. The interaction between the system and the reservoirs are denoted by the following sub-Hamiltonians

$H_{s-c} = \sum_k g_k\,(\hat{a}_k\,\hat{c}_k^\dagger + \hat{c}_k\,\hat{a}_k^\dagger)$ and $H_{s-m} = \sum_k f_k\,(\hat{b}_k\hat{m}_k^\dagger + \hat{b}_k^\dagger\hat{m}_k)$ (2)

where g_k or f_k is the bi-linear out-coupling function of traps A or B, respectively. The dynamical property of this system can be studied by solving the Heisenberg equation of motion $\frac{d\,\hat{O}}{dt} = -\frac{i}{\hbar}\,[\,\hat{O},\,\hat{H}\,]$, as shown in the textbooks [23,30]:

$\frac{d\hat{a}}{dt}$ = - $i\,\omega\,\hat{a} - i\,\Omega\,\hat{b}$- $i\,U\,\hat{a}^\dagger\hat{a}\,\hat{a} + \hat{F}_1$ (t) - $\int_0^t dt'$ $K(t\text{-}t')\,\hat{a}(t')$ (3)

$\frac{d\hat{b}}{dt}$ = - $i\,\omega\,\hat{b} - i\,\Omega\,\hat{a}$- $i\,U\,\hat{b}^\dagger\hat{b}\,\hat{b} + \hat{F}_2$ (t) - $\int_0^t dt'$ $M(t\text{-}t')\,\hat{b}(t')$ (4)

where $\hat{F}_1$ = - $i\sum_k g_k\,\hat{c_k}$ (0) $e^{-i\omega_k t}$ and $\hat{F}_2$ (t) = - $i\sum_k f_k\,\hat{c_k}$ (0) $e^{-i\omega_k t}$ correspond to the noise operators with reservoir variables. The last terms are the dissipation part with memory kernels $K(t) = \sum_k {g_k}^2\, e^{-i\omega_k t}$ and $M(t) = \sum_k {f_k}^2\, e^{-i\omega_k t}$. Applying OU memory kernels in the form $K(t) = Q_1\gamma\, e^{-\gamma t}$ and $M(t) = Q_2\gamma\, e^{-\gamma t}$ (OU referred to the authors of [31] who first used this function as memory kernel) attributes to the non-Markovian operational dynamics, whereas using memory-less kernels in the form K_δ(t)= $Q_1\,\delta(t)$ and M_δ(t)= $Q_2\,\delta(t)$ generates Markovian dynamics; see for example the works studied in [22, 26, 29, 32, 33].

3. The Dynamics of Mean-field Model (MF)

In general, there is no exact remedies for such non-linear operator equations, but an approximate solution can always be obtained by averaging them and decorrelating higher-order correlation operator functions into products of lower ones. In the present work, we decorrelate the third-order moment appearing on the right-hand side of Eqs. (3) and (4) by the relation:

$\langle a^\dagger aa\rangle \sim \langle a^\dagger\rangle\langle a\rangle\langle a\rangle$ and $\langle b^\dagger bb\rangle \sim \langle b^\dagger\rangle\langle b\rangle\langle b\rangle$. (5)

This means that third-order correlated operators are approximated by the product of their single-operator expectation values. This truncation is valid in the macroscopic limit, since the covariance vanishes as O($\frac{1}{N}$) (where N is the total number atom of the system) if the many-particle quantum state is close to pure BEC [2-4,14, 36, 37]. In other words, the mean-field approach is valid and well described for the macroscopic system (system with large number of atoms, $N \to \infty$).

The breakdown of mean-field model is by large, due to the neglect of higher order moments of the quantum state and not a consequence of a failure of the standard semi-classical Gross-Pitaevskii dynamics; see for example the discussion in the textbook of Pethick and Smith [34]. To overcome this problem, one has to truncate higher-order expectation values at a later stage than in Eq. (5)

$\langle a_j^\dagger a_k a_l\rangle \approx \langle a_j^\dagger\rangle\langle a_k a_l\rangle + \langle a_j^\dagger a_k\rangle\langle a_l\rangle + \langle a_j^\dagger a_l\rangle\langle a_k\rangle - 2\langle a_j^\dagger a_k a_l\rangle$ (6)

and derive the equation of motion for the correlation functions $\langle a_j^\dagger a_k\rangle$ and $\langle a_j a_k\rangle$, as suggested in [35]. However, this approach also finds its limitations and is later improved by the Bogoliubov back-reaction (BBR) method developed by Amichay Vardi's group [36].

Defining $\alpha = \langle\hat{a}\rangle$, $\alpha^* = \langle\hat{a}^\dagger\rangle$, $\beta = \langle\hat{b}\rangle$ and $\beta^* = \langle\hat{b}^\dagger\rangle$ with n(t)=$\alpha^2 + \beta^2 = n_A(t) + n_B$(t) denote the total particle number at a certain time t in the double-well. For large reservoir systems, averages $\langle\hat{F}_1\rangle$ and $\langle\hat{F}_2\rangle$ vanish. The Markovian operational dynamics of our model is obtained by choosing memory-less dissipation kernels K_δ(t) = $Q_1\,\delta(t)$ and M_δ(t) = $Q_2\,\delta(t)$ for Eqs. (3) and (4). We obtain the following set of coupled differential equations:

$\frac{d\alpha}{dt}$ = -$i\,(\omega - Q_1)\alpha$- $i\,\Omega\beta$-i U $|\alpha|^2\alpha$, (7)

$\frac{d\beta}{dt}$ = -$i\,(\omega - Q_2)\beta$-$i\,\Omega\alpha$- i U $|\beta|^2\beta$, (8)

Re-writing the variables (α, β) as $\alpha = |\alpha|exp\,(i\,\theta_a)$ and $\beta = |\beta|exp\,(i\,\theta_b)$, the population-imbalance parameter is defined by s = ($|\alpha|^2$-

$|\beta|^2$)/n(t) with a relative phase $\theta = \theta_a - \theta_b$. By calculating $\frac{ds}{dt} = \sum_j \frac{\partial s}{\partial \alpha_j}\frac{\partial \alpha_j}{\partial t}$, where $\alpha_j = \{\alpha, \beta\}$, and comparing the imaginary parts of $\frac{d(\alpha\beta^*)}{dt} = \frac{d(|\alpha||\beta|\exp(-i\theta))}{dt}$, one obtains the following set of equation:

$$\frac{ds}{dt} = -2\sqrt{1 - s^2}\sin\theta - \zeta(1 - s^2), \quad (9)$$

$$\frac{d\theta}{dt} = \frac{2s\cos\theta}{\sqrt{1-s^2}} - \chi s, \quad (10)$$

where $\zeta = (Q_2 - Q_1)/\Omega$ is the dissipation bias and $\chi = nU/\Omega$ is the ratio of inter-particle interaction with tunneling coupling strength. The model equations are then governed by the latter control parameters. Time has been rescaled in unit Ω. The fixed points are obtained by setting $(\dot{s} = 0, \dot{\theta} = 0)$; we obtain:

$$\sin\theta = \frac{\zeta}{2}\sqrt{1 - s^2} \text{ and } \cos\theta = \frac{\chi}{2}\sqrt{1 - s^2}\ . \quad (11)$$

Using trigonometry identity $\sin^2\theta + \cos^2\theta = 1$, we find $s = \pm\sqrt{1 - \frac{4}{\chi^2+\zeta^2}}$. Hence, we can identify the location of fixed points $(s, \theta) = (0, \arcsin\frac{\zeta}{2})$, $(0, \pi - \arcsin\frac{\zeta}{2})$, $(\sqrt{1 - \frac{4}{\chi^2+\zeta^2}}, \arccos\pi - \frac{\chi}{\chi^2+\zeta^2})$ and $(-\sqrt{1 - \frac{4}{\chi^2+\zeta^2}}, \arccos\pi - \frac{\chi}{\chi^2+\zeta^2})$.

Jacobian matrix for the non-dissipative two-mode BEC based on Eqs. (9) and (10) is as follows:

$$J = \begin{pmatrix} \frac{\partial \dot{s}}{\partial s} & \frac{\partial \dot{s}}{\partial \theta} \\ \frac{\partial \dot{\theta}}{\partial s} & \frac{\partial \dot{\theta}}{\partial \theta} \end{pmatrix} = \begin{pmatrix} 2s\sin\theta/\sqrt{1-s^2} - 2\zeta s & -2\sqrt{1-s^2}\cos\theta \\ -\chi + 2\cos\theta/\sqrt[3]{1-s^2} & -2s\sin\theta/\sqrt{1-s^2} \end{pmatrix} \quad (12)$$

3.1 Inter-particle Interaction and Dissipation Effect on the Mean-field System

We numerically solve Eqs. (9) and (10) [phase-space equations of the MF model] for appropriate initial conditions using Matlab ODE-45 solver [39, 40], which is an efficient tool for solving simple non-stiff differential equations. A relatively small number of atoms is used to maintain the validity of two-mode BEC model. For example, 100 atoms are distributed in appropriate proportions among the traps initially.

The population-imbalance invariant with control parameters (χ, ζ) is illustrated in Fig. 1. The left-most panels are evolutions for the dissipation free case. As the inter-particle interaction increases, one observes phase changes from Quantum Tunneling state (QTS) to Macroscopic Self-trapping state (MQST). In the transition from MQST to Josephson oscillations (as the atom numbers are dropping), one sees something like "periodic doubling" (blue curve in the figure). One could expect some sort of resonance to occur as the system's phases change from QTS to MQST as one sweep through from weak to stronger non-linearity.

The middle and right-most panels of Fig. 1 are the dynamics in the presence of dissipation. Competition between atom tunneling and atom losses to the reservoir is seen to be affecting the dynamics. Comparing the evolution of figures between these two sets of panels, one can deduce that stronger dissipation coupled with inter-particle interaction causes dramatic changes in the dynamics of the system (irregular reduction in the population-imbalance oscillation amplitude). In other words, dissipation has perturbed the period-doubling effect and starts delocalizing atoms (damped oscillation) as the atom number drops. However, for the strongly inter-particle interacting case, in the last bottom left panels, dissipation is seen to drive back MQST to QTS, as the non-linearity of the system gets weaker in proportion to reducing atom number.

Stability characteristics of the fixed points can be determined by finding the eigenvalues of the Jacobian matrix, as shown in the differential equations textbooks [41, 42]. It was also shown by the researchers in [3, 14, 43] that the eigenvalues of the Jacobian matrix depict the type of fixed points and the stability of them. For instance, two imaginary eigenvalues denote an elliptic fixed point, two real eigenvalues denote a hyperbolic fixed point. A saddle fixed point occurs when two real eigenvalues lie on the different sides of zeros. Complex eigenvalue with a negative real part depicts an attractor, while a complex eigenvalue with positive real part depicts a repeller.

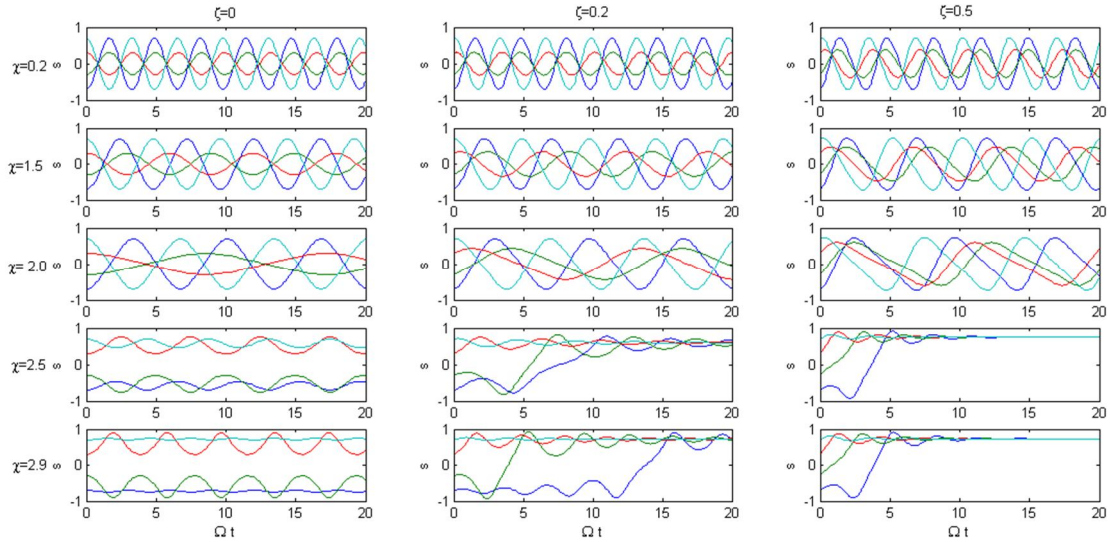

FIG. 1. Evolution of population imbalance s as a function of Ωt in variation with dissipation strengths ζ for various inter-particle interaction strengths χ. Phases are evolving from Quantum Tunneling state (QTS) (Josephson's oscillations) at χ = 0.2 to Macroscopic Quantum Self-trapping (partially localized oscillations) at χ=2.5 onward. Coloured lines correspond to initial conditions (s(0), $\theta(0)$): (-0.7,0) blue-line, (-0.3,0) green line, (0.3,0) red-line and (0.7,0) light-blue line.

Fig. 2 shows a comparison of dissipative and dissipation-free phase space trajectory (s, θ) evolutions in variation with inter-particle interaction strengths (increasing from top to bottom order). Phases are evolving from Quantum Tunneling state (QTS) (all elliptic fixed points) at χ = 0.2 to Macroscopic Quantum Self-trapping (MQST) state (a combination of hyperbolic and elliptic fixed points) at χ = 2.0 onwards. The middle and right-most panels show perturbation to phases shown in the left panel in the presence of dissipation. Top left-most panel of Fig. 2 depicts the phase diagram for the weak on-site interaction χ = 0.2. Three elliptic fixed points at locations (s, θ) = (0, $\pm\pi$), (0,0) are easily noticeable for the dissipation-free case. The effect of dissipation is noticeable at theχ middle (ζ= 0.2) and right-most panels (ζ=0.5) of Fig. 2. The presence of dissipation causes the pair of elliptic fixed points to be attracted to each other. Also, there is a slight shift in the locations of the fixed points.

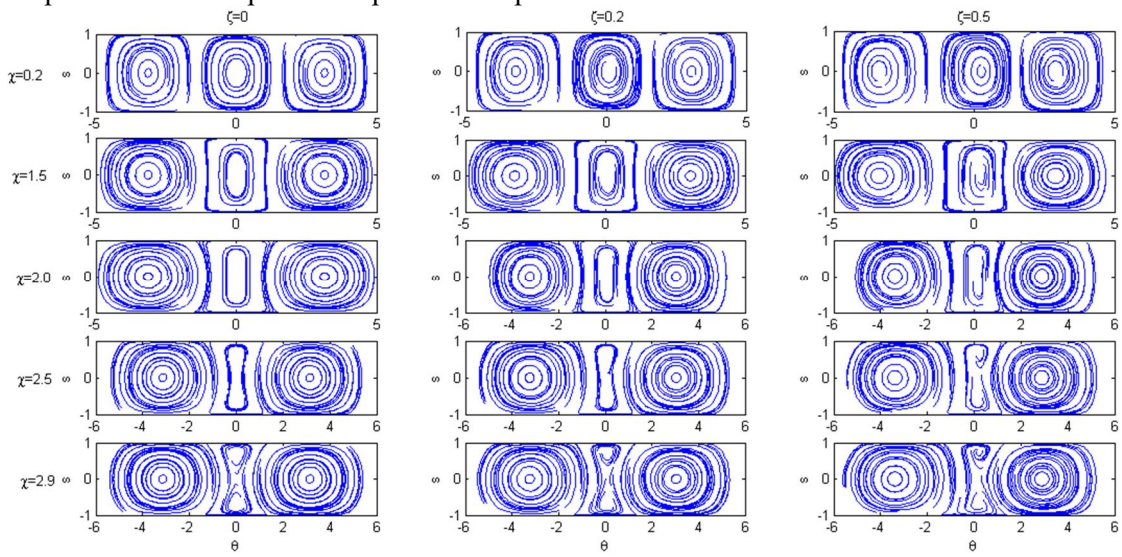

FIG. 2. Evolution of phase diagrams (s, θ) in variation with inter-particle interaction strengths (increasing χ from top to bottom order) subjected to three dissipation strengths ζ=0,0.2,0.5. Initial conditions are in the ranges $-1 \leq s(0) \leq 1$ and $-\pi \leq \theta(0) \leq \pi$ while the trajectories run for Ωt=3. Phases are evolving from Quantum Tunelling state (QTS) (all elliptic fixed points) at χ=0.2 to Macroscopic Quantum Self-trapping state (a combination of hyperbolic and elliptic fixed points) at χ=2.5 onward corresponding to Figure 2. Phase difference, θ, is plotted in unit radian.

Looking at the horizontal row of panels with χ = 2.5, the phase diagram clearly exhibits two elliptic fixed points at (s, θ) = (0, -π), (0, π) and a single hyperbolic fixed point at (0,0) for the dissipation-free case (left-most panel). In the strongly interacting case without dissipation, one observes the splitting of one of the elliptic fixed points into two novel elliptic points and one hyperbolic fixed point; this is the famous self-trapping effect reported by Milburn et al. [2], Raghavan et al. [4] and observed experimentally by Albiez et al. [5]. Dissipation introduced in the system (right-most panel of Fig. 2) generates a pair of attractor and repeller at (0.6, 0) and (-0.6, 0), respectively. There is no change of location for the other two fixed points, but the dynamics can be seen to be corrugated by the presence of dissipation.

Bottom-most Fig. 2 is the phase portrait for stronger on-site interaction χ = 2.9. A corrugated hyperbolic fixed point at (0, 0) and two elliptic fixed points at (0, $\pm\pi$) were found for the non-dissipative case (the last row left-most panel). The system generates four fixed points for the dissipation case (last row of middle and right-most panels). The fixed points are located at ($\pm$ 0.72, 0) and (0, $\pm\,\pi$). Fixed points at (0.72, 0) are attractors, while the ones at (-0.72,0) are repellers. The other two fixed points at (0, $\pm\pi$) are elliptic. The above stability characteristics of fixed points are deduced from the eigenvalue result of its Jacobian matrix.

4. The Fluctuation-dissipation Noise Correlated (FDT) Model

There are shortcomings for the use of mean-field approximation. For instance, quantum fluctuations are completely neglected and they also fail badly at dynamical instabilities [35]. Also, the system noise is suppressed since the thermal noise expectation value $\langle F_j^{\dagger}(t)\rangle$ = $\langle F_j(t)\rangle$ = 0 assuming a large thermal reservoir. Hence, noise correlation effects are completely neglected in the system. In this work, we implement the double-well BEC system subjected to noise correlation and Markovian dissipation. We call this description the FDT model.

Physical quantities, such as population of traps ($n_A = \langle \hat{a}^{\dagger}\,\hat{a}\rangle$, $n_B = \langle \hat{b}^{\dagger}\hat{b}\,\rangle$), coherence and other noise-correlated terms, are computed by their second-order moments using Eqs. (3) and (4) and applying the product rule: $\frac{d\langle \hat{O}^{\dagger}\,\hat{O}\rangle}{dt}$ = $\langle \frac{d\hat{O}}{dt}\,\hat{O}\rangle + \langle \hat{O}\,\frac{d\hat{O}}{dt}\rangle$. Performing some algebra, we obtain the following set of second-order moment evolution equations:

$$\frac{d\langle \hat{a}^{\dagger}\hat{a}\rangle}{dt} = -2\,Q_1\,\langle \hat{a}^{\dagger}\,\hat{a}\rangle + i\,\Omega\,\langle \hat{b}^{\dagger}\hat{a}\rangle - i\,\Omega\,\langle \hat{a}^{\dagger}\hat{b}\rangle + \langle \hat{F}_1^{\dagger}\,\hat{a}\,\rangle + \langle \hat{a}^{\dagger}\,\hat{F}_1\rangle \quad (13)$$

$$\frac{d\langle \hat{b}^{\dagger}\hat{b}\rangle}{dt} = -2\,Q_2\,\langle \hat{b}^{\dagger}\,\hat{b}\rangle + i\,\Omega\,\langle \hat{a}^{\dagger}b\rangle - i\,\Omega\,\langle \hat{b}^{\dagger}\hat{a}\rangle + \langle \hat{F}_2^{\dagger}\,\hat{b}\,\rangle + \langle \hat{b}^{\dagger}\,\hat{F}_2\rangle \quad (14)$$

$$\frac{d\langle \hat{a}^{\dagger}\hat{b}\rangle}{dt} = -\,(Q_1{+}Q_2\,)\;\;\langle \hat{a}^{\dagger}\,\hat{b}\rangle + i\,\Omega\,\langle \hat{b}^{\dagger}\hat{b}\rangle - i\,\Omega\,\langle \hat{a}^{\dagger}\hat{a}\rangle + iU\,\langle a^{\dagger}\,\hat{b}\,\rangle\,(n_A - n_B). \quad (15)$$

The noise terms in the above equations denoted by ($\hat{F}_1$, $\hat{F}_2$) obey the two-point correlations relation; see for example [23, 28]:

$$\langle \hat{F}_1(t')\,\hat{F}_2(t'')\rangle = Q_1\,N_1(\omega)\,\delta(\,t'-t") \quad (16)$$

$$\langle \hat{F}_1(t')\,\hat{F}_2(t'')\rangle = Q_2\,N_2(\omega)\,\delta(\,t'-t") \quad (17)$$

It needs to be mentioned that Eqs. (16) and (17) indicate Fluctuation-Dissipation theorem (FDT) for the Markovian system [for non-Markovian system, we have different relations than those above], which reads that fluctuation-due reservoir contributes to the dissipation in the system. In the above set of equations, the terms $\langle \hat{F}_1^{\dagger}\,\hat{a}\,\rangle = \langle \hat{a}^{\dagger}\,\hat{F}_1\rangle = (Q_1/2)\;N_1(\omega)$ and $\langle \hat{F}_2^{\dagger}\,\hat{b}\,\rangle = \langle \hat{b}^{\dagger}\,\hat{F}_2\rangle = (Q_2/2)\;N_2(\omega)$ were obtained using Eqs. (16) and (17) and employing the technique shown in the textbook [28].

The fourth-order moments generated in deriving Eqs. (13) - (15) have been de-correlated by a basic relation $\langle \hat{A}\,\hat{B}\hat{C}\hat{D}\,\rangle \approx \langle \hat{A}\hat{B}\rangle\langle \hat{C}\hat{D}\rangle$. The set of dynamical equations above are governed by the trap frequency ω, tunneling coupling constant Ω, inter-particle interaction strength U, dissipation strengths (Q_1, Q_2) and the reservoir temperatures (T_1, T_2).

4.1 Comparison between the MF and FDT Models and Their Illustrations

We compare the FDT model Eqs. (13) - (15) with MF model Eqs. (7) and (8) in terms of their physical quantities, such as population imbalance, coherence and entanglement. Again, we distribute 100 atoms in appropriate proportions among the traps as their initial condition. The trap frequency is set at ω/Ω = 5. Dissipation strengths (Q_1, Q_2) and the ratio

between inter-particle interaction with tunneling strength U/Ω are treated as control parameters for the system dynamics. Reservoir temperatures are fixed at $k_B T_1/\Omega = k_B T_2/\Omega = 2$, while the trap frequency is set at $\omega/\Omega = 5$.

4.1.1 Population Imbalance

The non-dissipative two-mode BEC exhibits quantum tunneling state (QTS) at weaker inter-particle interaction as can be noticed in Fig. 3(a), while a macroscopic self-trapping state (MQST) is realized in Fig. 3(b) for a stronger interaction regime [2, 4]. The population imbalance at QTS displays Rabi Josephson oscillation, whereas MQST shows partially localized oscillation.

Fig. 3(b) shows decaying oscillation and continuous reduction of population amplitude. The QTS phase is destroyed by dissipation in both models. Fig. 3(d) indicates a drive back from MQST to QTS. The MF model drives the system quicker to its equilibrium state compared to the FDT model. As the atom numbers are dropping, one sees something like a "period doubling" for the FDT model. The slower decay into the equilibrium for the FDT model is due to noise and dissipation in the system, sustaining the dynamics.

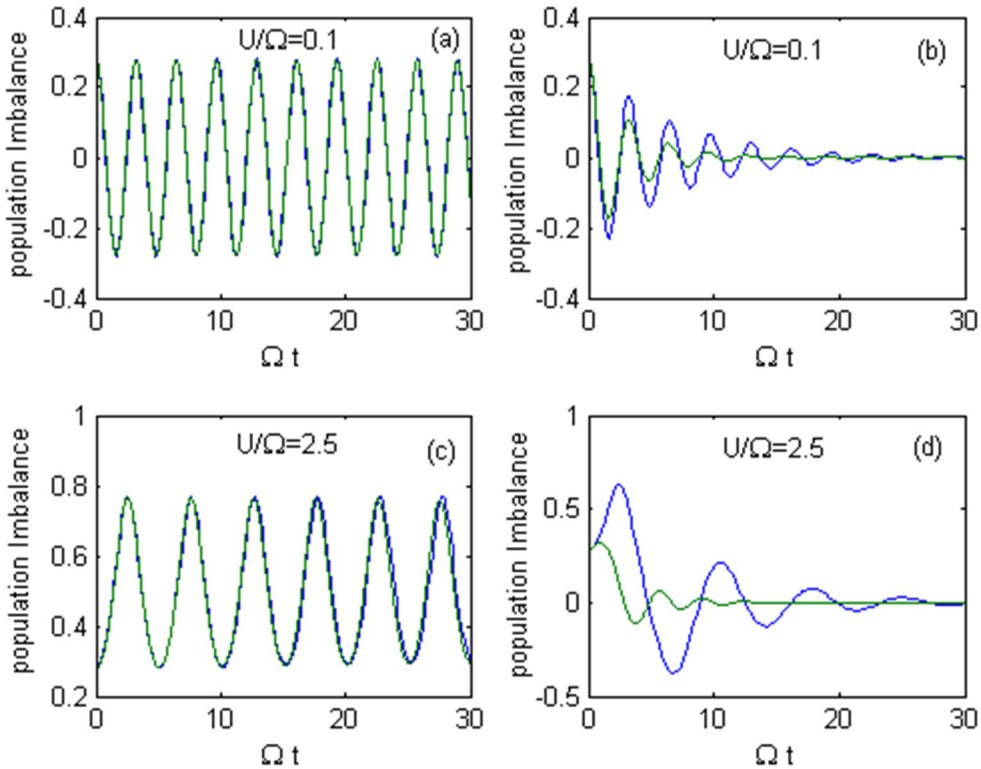

FIG. 3. Population imbalance as a function of Ωt. Top panels are for weak inter-particle interaction strength U/Ω = 0.1, while lower panels are for its stronger counterpart U/Ω = 2.5. Figs. (a) and (c) correspond to non-dissipative dynamics representing QTS and MQST, respectively. Figs. (b) and (d) are their corresponding system with dissipation strength Q_1/Ω=0.1 and Q_2/Ω=0.2. Other fixed parameters are trap frequencies ω/Ω=5 and reservoir temperatures $k_B\ T_1/\Omega$=2 and $k_B\ T_2/\Omega$=2 . Initial atom distribution for traps (A, B) is (64, 36). The blue line corresponds to the noise-correlated (FDT) model, while the green line is for the MF model.

4.1.2 Coherence in the System

The coherence of the many-body quantum state can be determined using the first-order correlation function between wells $g_{ab}^{(1)} = \left[\langle \hat{a}^\dagger \hat{b}\rangle + \langle \hat{b}^\dagger \hat{a}\rangle\right]/n(t)$ [13]. We compare the coherence produced by the two models (FDT *vs.* MF) in Fig. 4 for various inter-particle interaction strengths.

The MF model shows a sharp exponential decay of coherence in the traps for this weak inter-particle interaction limit $U \leq 2\Omega$. The FDT model, however, sustains stable coherence for this range of interaction strength, maintaining pure condensate state. This interesting feature, we believe, is due to the balance between noise and dissipation factor that is peculiar to the system, supporting fluctuation dissipation theorem.

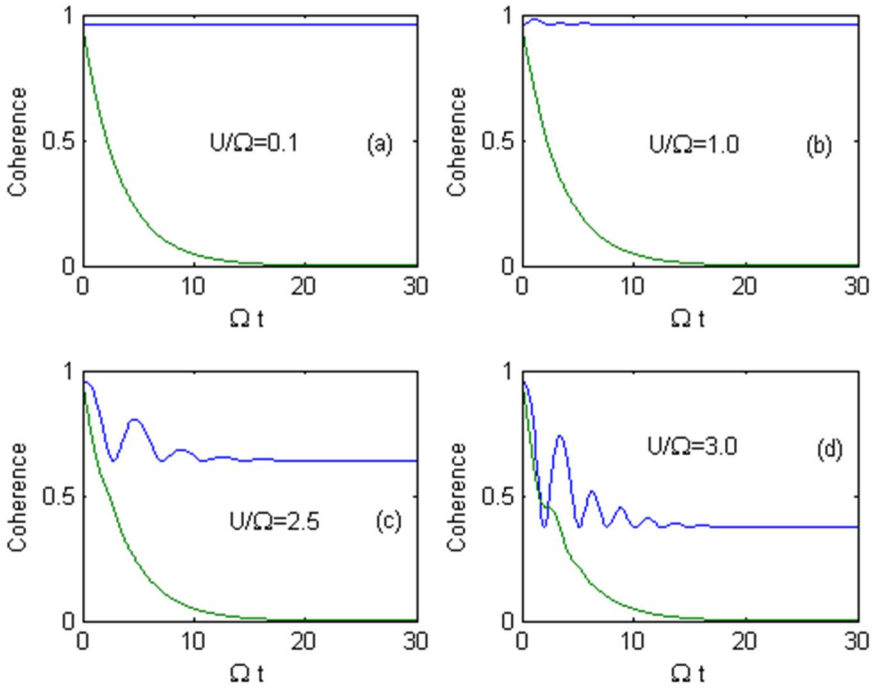

FIG. 4. Coherence dynamics as a function of Ωt computed in variation with the inter-particle interaction strength U/Ω. Trap frequencies, reservoir temperatures, dissipation strengths and initial atom distribution at traps (A,B) are the same as in Figure 3. Blue and green lines correspond to the noise-correlated Markovian model and the mean-field model (MF), respectively.

We found that dissipation drives the initial state of the system to a different quantum state for the stronger inter-particle interaction regimes $U \geq 2.5\ \Omega$. In this limit, both models show a decrease in the first-order coherence, indicating the destruction of the condensate. The initial state of the systems is unstable; they fragmented into a meta-stable equilibrium state, similarly reported by Kordas et al. [44]. The sudden jump to a local maximum coherence after a short transient period is understood to be a stochastic resonant (SR) effect reported by Witthaut et al. (2008) [13]. Such phenomena occur for dissipative systems at a stronger non-linear interaction only.

The MF model also exhibits similar transient BEC fragmentation and formation of resonant state, but cannot sustain it, as the coherence decays sharply. However, the FDT model based on noise and dissipation balancing supports the meta-stable equilibrium for longer sustainable periods. The oscillatory dynamics in Fig. 4 (c) and (d) for the FDT model is due its competition between dissipation and atom losses, which eventually creates the meta-stable state.

4.1.3 Entanglement

To investigate the inter-modal entanglement between BEC atoms, we use the Hillery-Zubairy criteria [45, 46] defined by the following relations, $HZ1 = \langle \hat{n}_A\, \hat{n}_B \rangle - \left|\langle \hat{a}^\dagger \hat{b} \rangle\right|^2$ or $HZ2 = \langle \hat{n}_A \rangle \langle \hat{n}_B \rangle - \left|\langle \hat{a}\hat{b} \rangle\right|^2$ for which $HZ1 < 0$ or $HZ2 < 0$, indicating entanglement. HZ1 criterion is the suitable candidate for our models; therefore, it is plotted in Fig. 5.

Interestingly, the domain of non-classicality (entanglement) detected through HZ1 criterion depends on the ratio of non-linear interaction and coherence. The MF model does not show entanglement, because equation HZ1 is zero based on its decorrelation approximation and mean-field definition. In this situation, the system remains close to pure BEC throughout its evolution. FDT model is highly entangled even at weak interaction. For weak interaction, higher atom-tunneling rate enhances coherence in the system. However, the atom-density fluctuations at each trap weakened by atom losses to the reservoir (referring to equation HZ1). We have mentioned earlier that coherence is sustained by the FDT model, which supports our argument. The BEC was fragmented into meta-stable equilibrium state for stronger inter-particle interaction ($U \geq 2.5\ \Omega$). Such phenomena are also captured by the entanglement evolution shown in Fig. 4 (c) and Fig. 4 (d).

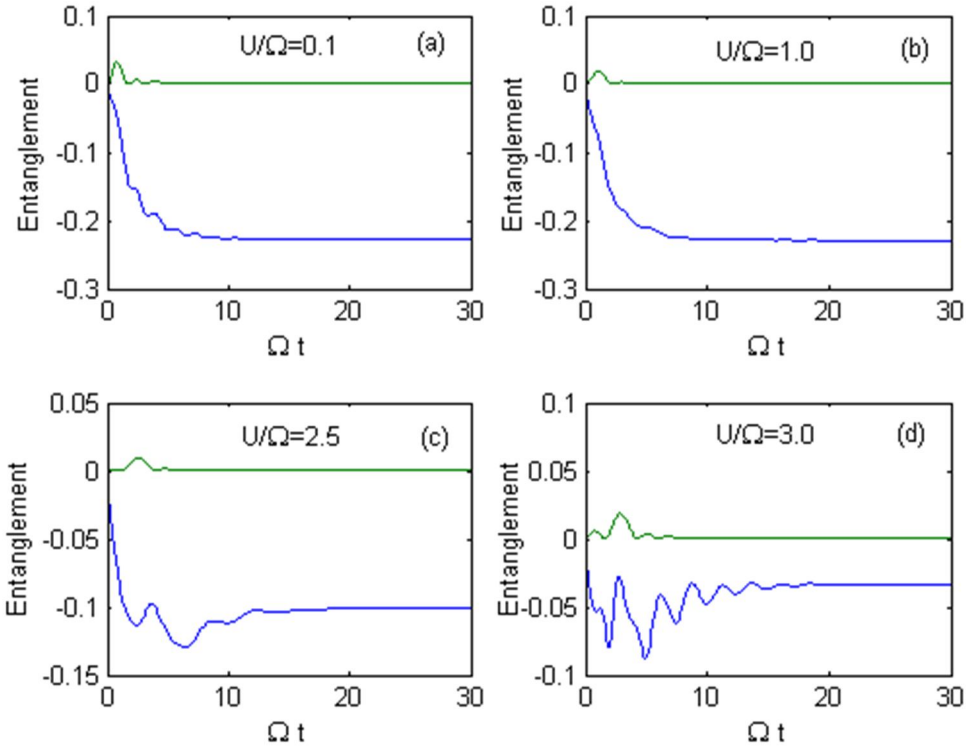

FIG. 5. HZ-1 criterion in the time domain Ωt for various inter-particle interaction strengths. Caption is still the same as in Figure 3.

5. Conclusion

We have studied the dynamical properties of a double-well BEC out-coupled to a dual-reservoir system. Dissipation in the system arises from the interaction of condensate atoms with the out-coupled multi-mode reservoirs. The macroscopic dynamics of BEC modes are described within the mean-field and noise-correlated models.

We started by analyzing the dynamics induced by the mean-field model (MF) subjected to Markovian dissipation. We have shown how the system evolved from its initial equilibrium phases (QTS and MQST) and perturbed in variation with the applied control parameters (non-linear interaction and dissipation strengths). Later, we considered the noise-correlated model (FDT) and computed the physical quantities, such as population imbalance, coherence and entanglement. The FDT model obeys the fluctuation dissipation theorem, which recognizes fluctuation in the reservoir as the main source of dissipation in the system. However, the noise correlation is suppressed in the MF model.

We have shown that noise correlation and dissipation have crucial effects on computing physical quantities, such as population imbalance, coherence or entanglement of the system. Dissipation destroys the two-mode BEC phases; namely, QTS and MQST, which occur at the opposite interacting regimes (weak *versus* strong). Coherence of the system is enhanced for weaker non-linear interaction strength (due to increasing tunneling rate), hence promoting non-classical (quantum) behavior. Dissipation drives back MQST to QTS phase reaching a meta-stable state before being destroyed, as the non-linearity of the system gets weaker in proportion to reducing atom number. The mentioned process is much weaker and slower in the FDT model compared to the MF model.

The present work opens up a new research direction to analyze possible formation of non-linear structures, like the breather state (especially at stronger non-linear interaction and dissipation regime) similar to the system studied by Kordas et al. [44]. We have shown that the mean-field model (where noise correlation is suppressed) is not able to detect quantum properties, like coherence and entanglement, especially at the stronger non-linear interaction and dissipation regime, where new quantum features emerge. We hope that the formation of breather state is also realized in experiment using a simple system like our double-well BEC-reservoir models.

Acknowledgement

The present research was initially supported by the National Fundamental Research Grant Scheme FRGS of Malaysia, 01-01-17-1921FR. Part of the work was presented at "ICRAAM 2020" Conference held at Kuala Lumpur on 4th - 6th February 2020. We highly appreciate the deep and insightful comments of our reviewers in improving the content of this manuscript.

Appendix: The Mean-field Non-Markovian Dynamics

The non-Markovian operational dynamic model is obtained by choosing memory dissipation kernels K_1 (t) = Q_1 exp (-γ t) and M_1(t) = Q_2 exp(-γ t) for Eqs. (3) and (4). Following the prescribed steps in Section 3, we obtain the mean-field set of coupled differential equations:

$$\frac{d\alpha}{dt} = -i\omega\alpha - i\Omega\beta - iU|\alpha|^2\alpha - Q_1\int_0^t dt' \exp(-\gamma[t-t'])\,\alpha(t'), \quad \text{(A1)}$$

$$\frac{d\beta}{dt} = -i(\omega)\beta - i\Omega\alpha - iU|\beta|^2\beta - Q_2\int_0^t dt' \exp(-\gamma[t-t'])\beta(t'). \quad \text{(A2)}$$

The following are the set of phase-space dynamical equations for our non-Markovian system:

$$\frac{ds}{dt} = -2\sqrt{1-s^2}\sin\theta - \zeta(1-s^2) - \left[\frac{1+s}{n}\right][\beta^* Y + \beta Y^*] - \left[\frac{1-s}{n}\right][\alpha^* X + \alpha X^*] \quad \text{(A3)}$$

$$\frac{d\theta}{dt} = \frac{2s\cos\theta}{\sqrt{1-s^2}} - \chi s - \Im\left\{\frac{Y^*}{\beta^*} + \frac{X}{\alpha}\right\}, \quad \text{(A4)}$$

where $\Im$ stands for the imaginary part. In the above equations, the non-local memory kernel terms are represented by new variables:

$$X(t) = -Q_1\int_0^t dt' \exp(-\gamma[t-t'])\,\alpha(t') \quad \text{(A5)}$$

$$Y(t) = -Q_2\int_0^t dt' \exp(-\gamma[t-t'])\beta(t') \quad \text{(A6)}$$

Satisfying

$$\dot{X} = \gamma X(t) - \gamma Q_1 \alpha(t) \quad \text{(A7)}$$

$$\dot{Y} = \gamma Y(t) - \gamma Q_1 \beta(t). \quad \text{(A8)}$$

The phase-space variables (s, θ) are not in closed form; they require extra variables (α, β,X, Y). Hence, we need to solve a higher-dimensional non-linear problem now. The six-dimensional equilibrium point is determined by setting $(\dot{\alpha}=0, \dot{\beta}=0, \dot{s}=0, \dot{\theta}=0, \dot{X}=0, \dot{Y}=0)$. We start by solving the simplest equation first. Eqs. (A7) and (A8) lead to the solution $X_j = -Q_1\alpha_j$ and $Y_j = -Q_2\beta_j$. Substitution into Eq. (A3) and Eq. (A4) leads to obtain the following relations:

$$\sin\theta_j = \frac{\zeta}{2}\sqrt{1-s_j^2} \quad \text{(A9)}$$

$$\cos\theta_j = \frac{\chi}{2}\sqrt{1-s_j^2} \quad \text{(A10)}$$

$$s_\pm = \pm\sqrt{1-\frac{4}{\chi^2+\zeta^2}} \quad \text{(A11)}$$

where the control parameters are $\zeta = (Q_2 - Q_1)/\Omega$ and $\chi = nU/\Omega$. The four fixed points (in six-dimensional space) are $P_{j=1,2,3,4} = (\alpha_j, \beta_j, X_j, Y_j, s_j, \theta_j)$:

$$P_1 = (\alpha_1, \beta_1, -Q_1\alpha_1, -Q_2\beta_2, 0, \sin^{-1}\frac{\zeta}{2}),$$

$$P_2 = (\alpha_2, \beta_2, -Q_1\alpha_2, -Q_2\beta_2, 0, \pi - \sin^{-1}\frac{\zeta}{2}),$$

$$P_3 = (\alpha_3, \beta_3, -Q_1\alpha_3, -Q_2\beta_3, \sqrt{1-\frac{4}{\chi^2+\zeta^2}}, \pi - \cos^{-1}\frac{\chi}{\chi^2+\zeta^2})$$

and

$$P_4 = (\alpha_4, \beta_4, -Q_1\alpha_4, -Q_2\beta_4, -\sqrt{1-\frac{4}{\chi^2+\zeta^2}}, \pi - \cos^{-1}\frac{\chi}{\chi^2+\zeta^2})$$

where (α_j, β_j) are obtained by solving the following non-linear coupled equations:

$$(-i\,\omega - Q_1 - i\,U\,|\alpha_j|^2)\,\alpha_j - i\,\Omega\,\beta_j = 0 \quad \text{(A12)}$$

$$-i\,\Omega\,\alpha_j + (-i\,\omega - Q_2 - i\,U\,|\beta_j|^2)\,\beta_j = 0. \quad \text{(A13)}$$

The above set of equations was derived from $\dot{\alpha} = 0$ and $\dot{\beta} = 0$ of Eqs. (A1) and (A2). The stability characteristic of the system has to be solved by 6 × 6 Jacobian matrix applying fixed points P_j. The Jacobian matrix is:

$$Z = \begin{pmatrix} z_{11} & -i & 1 & 0 & 0 & 0 \\ -i & z_{22} & 0 & 0 & 0 & 0 \\ -Q_1\alpha & 0 & -\gamma & 0 & 0 & 0 \\ 0 & -Q_2\beta & 0 & -\gamma & 0 & 0 \\ z_{51} & z_{52} & z_{53} & z_{54} & z_{55} & z_{56} \\ z_{61} & 0 & z_{63} & 0 & z_{65} & z_{66} \end{pmatrix} \quad \text{(A14)}$$

where $z_{11} = -i\omega - 2iU|\alpha|^2$, $z_{22} = -i\omega - 2iU|\beta|^2$, $z_{51} = \frac{1-s}{n}X^*$, $z_{52} = -\frac{1+s}{n}Y^*$,

$z_{53} = \frac{1-s}{n}\alpha^*$, $z_{54} = -\frac{1+s}{n}\beta^*$, $z_{55} = \frac{2s}{\sqrt{1-s^2}}\sin\theta - \frac{\alpha^*X+\alpha X^*}{n} - \frac{\beta^*Y+\beta Y^*}{n}$, $z_{56} = \frac{-2s\,\cos\theta}{\sqrt{1-s^2}}$, $z_{61} = -\Im\left(-\frac{X}{\alpha^*}\right)$, $z_{63} = \Im\left(\frac{1}{\alpha}\right)$, $z_{65} = \frac{2\cos\theta}{\sqrt[3]{1-s^2}} - \chi$ and $z_{66} = \frac{-2\,s\,\sin\theta}{\sqrt{1-s^2}}$.

For example, we can test the above result for interaction-free (χ= 0), dissipative (ζ = 0.1) systems, with other given parameters ω = 2.0, γ = 10, $Q_2 = 0.2$ and Q_1 =0.1, which takes a fixed point P_1 = (0, 0, 0, 0, 0, 0.05); thus, we have:

$$Z_{P1} = \begin{pmatrix} -2i & -i & 1 & 0 & 0 & 0 \\ -i & -2i & 0 & 0 & 0 & 0 \\ -1 & 0 & -10 & 0 & 0 & 0 \\ 0 & -2 & 0 & -10 & 0 & 0 \\ 0 & 0 & 0 & 0 & 0 & 0 \\ 0 & 0 & 0 & 0 & 2 & 0 \end{pmatrix} \quad \text{(A15)}$$

which gives a set of eigenvalues (-0.19 - 3.06i, -0.20 - 1.02i, -9.80 + 0.02i, -9.81+ 0.06i, 0, 0) that verifies a damped oscillatory motion of the system.

References

[1] Javanainen, J., Physical Review Letters, 57 (25) (1986) 3164.

[2] Milburn, G.J., Corney, J.F., Wright, E.M. and Walls, D.F., Physical Review A, 55 (6) (1997) 4318.

[3] Smerzi, A., Fantoni, S., Giovanazzi, S. and Shenoy, S.R., Physical Review Letters, 79 (25) (1997) 4950.

[4] Raghavan, S., Smerzi, A., Fantoni, S. and Shenoy, S.R., Physical Review A, 59 (1) (1999) 620.

[5] Albiez, M., Gati, R., Froelling, J., Hunsmann, S., Cristiani, M. and Oberthaler, M.K., Physical Review Letters, 95 (1) (2005) 010402.

[6] Gati, R., Hemmerling, B., Froelling, J., Albiez, M. and Oberthaler, M.K., Physical Review Letters, 96 (13) (2006) 130404.

[7] Zibold, T., Nicklas, E., Gross, C. and Oberthaler, M.K., Physical Review Letters, 105 (20) (2010) 204101.

[8] Levy, S., Lahoud, E., Shomroni, I. and Steinhauer, J., Nature, 449 (7162) (2007) 579.

[9] Hofferberth, S., Lesanovsky, I., Schumm, T., Imambekov, A., Gritsev, V., Demler, E. and Schmiedmayer, J., Nature-Physics, 4 (6) (2008) 489.

[10] Ruostekoski, J. and Walls, D.F., Physical Review A, 58 (1) (1998) R50.

[11] Khodorkovsky, Y., Kurizki, G. and Vardi, A., Physical Review Letters, 100 (22) (2008) 220403.

[12] Boukobza, E., Chuchem, M., Cohen, D. and Vardi, A., Physical Review Letters, 102 (18) (2009) 180403.

[13] Witthaut, D., Trimborn, F. and Wimberger, S., Physical Review Letters, 101 (20) (2008) 200402.

[14] Trimborn, F., Witthaut, D. and Wimberger, S., Journal of Physics B: Atomic, Molecular and Optical Physics, 41 (17) (2008) 171001.

[15] Witthaut, D., Trimborn, F., and Wimberger, S., Physical Review A, 79 (3) (2009) 033621.

[16] Wang, W., Fu, L.B. and Yi, X.X., Physical Review A, 75 (4) (2007) 045601.

[17] Huang, Y., Tan, Q.S., Fu, L.B. and Wang, X., Physical Review A, 88 (6) (2013) 063642.

[18] Ghasemian, E. and Tavassoly, M.K., Physics Letters A, 380 (40) (2016) 3262.

[19] Ghasemian, E. and Tavassoly, M.K., Laser Physics, 27 (9) (2017) 095202.

[20] Guarrera, V., Wuertz, P., Ewerbeck, A., Vogler, A., Barontini, G. and Ott, H., Physical Review Letters, 107 (16) (2011) 160403.

[21] Barontini, G., Labouvie, R., Stubenrauch, F., Vogler, A., Guarrera, V. and Ott, H., Physical Review Letters, 110 (3) (2013) 035302.

[22] Lindenberg, K. and West, B.J., "The Non-equilibrium Statistical Mechanics of Open and Closed Systems", (VCH New York, 1990).

[23] Scully, M.O. and Zubairy, M.S., "Quantum Optics", (Cambridge University Press, 1997).

[24] Lazarou, C., Nikolopoulos, G.M. and Lambropoulos, P., Journal of Physics B: Atomic, Molecular and Optical Physics, 40 (12) (2007) 2511.

[25] Nikolopoulos, G.M., Lazarou, C. and Lambropoulos, P., Journal of Physics B: Atomic, Molecular and Optical Physics, 41 (2) (2008) 025301.

[26] Rajagopal, K.K., Physica A: Statistical Mechanics and Its Applications, 429 (5) (2015) 231.

[27] Rajagopal, K.K. and Muniandy, S.V., Physica A: Statistical Mechanics and Its Applications, 434 (2015) 164.

[28] Yamamoto, Y. and Imamoglu, A., "Mesoscopic Quantum Optics", (John Wiley & Sons, Inc., New York, 1999).

[29] Rajagopal, K.K. and Ibragimov, G., Brazilian Journal of Physics, 50 (2) (2020) 178.

[30] Weiss, U., "Quantum Dissipative Systems", 3rd Edition, (World Scientific, Singapore, 2008).

[31] Uhlenbeck, G.E. and Ornstein, L.S., Physical Review, 36 (1930) 823.

[32] Sargsyan, V.V., Adamian, G.G., Antonenko, N.V. and Lacroix, D., Physical Review A, 90 (2) (2014) 022123.

[33] Rajagopal, K.K. and Ibragimov, G., Brazilian Journal of Physics, 51 (2021) 944.

[34] Pethick, C.J. and Smith, H., "Bose-Einstein Condensation in Dilute Gases", (Cambridge University Press, 2008).

[35] Trimborn, F., Witthaut, D. and Korsch, H.J., Physical Review A, 79 (1) (2009) 013608.

[36] Anglin, J.R. and Vardi, A., Physical Review A, 64 (1) (2001) 013605.

[37] Vardi, A, Yurovsky, V.A. and Anglin, J.R., Physical Review A, 64 (6) (2001) 063611.

[38] Tikhonenkov, I., Anglin, J.R. and Vardi, A., Physical Review A, 75 (1) (2007) 013613.

[39] Constantinides, A. and Mostoufi, N., "Numerical Methods for Chemical Engineers with Matlab Applications with Cdrom", (Prentice Hall PTR, 1999).

[40] Shampine, L.F., Gladwell, I., Shampine, L. and Thompson, S., "Solving ODEs with Matlab", (Cambridge University Press, 2003).

[41] Perko, L., "Differential Equations and Dynamical Systems", Volume 7, (Springer Science & Business Media, 2013).

[42] Barreira, L. and Valls, C., "Dynamical Systems: An Introduction", (Springer Science & Business Media, 2012).

[43] Bo, C., Lin, W.S. and Xi, Y.X., Chinese Physics Letters, 27 (7) (2010) 070303.

[44] Kordas, G., Wimberger, S. and Witthaut, D., Physical Review A, 87 (4) (2013) 043618.

[45] Hillery, M. and Zubairy, M.S., Physical Review Letters, 96 (5) (2006) 050503.

[46] Hillery, M. and Zubairy, M.S., Physical Review A, 74 (3) (2006) 032333.

[47] Labouvie, R., Santra, B., Heun, S., Wimberger, S. and Ott, H., Physical Review Letters, 115 (2015) 050601.

[48] Labouvie, R., Santra, B., Heun, S., Wimberger, S. and Ott, H., Physical Review Letters, 116 (2016) 235302.

[49] Kosloff, R., Quantum Thermodynamics: Entropy, 15 (2013) 2100.

[50] Hofer, P.P., Perarnau-Llobet, M., Miranda, L.D.M., Haack, G., Silva, R., Brask, J.B. and Brunner, N., New Journal of Physics, 19 (12) (2017) 123037.